

## Equilibrium cluster formation and gelation

This article has been downloaded from IOPscience. Please scroll down to see the full text article.

2005 J. Phys.: Condens. Matter 17 S3551

(<http://iopscience.iop.org/0953-8984/17/45/047>)

View [the table of contents for this issue](#), or go to the [journal homepage](#) for more

Download details:

IP Address: 129.252.86.83

The article was downloaded on 28/05/2010 at 06:43

Please note that [terms and conditions apply](#).

# Equilibrium cluster formation and gelation

Rodrigo Sanchez and Paul Bartlett

School of Chemistry, University of Bristol, Bristol BS8 1TS, UK

E-mail: [P.Bartlett@bristol.ac.uk](mailto:P.Bartlett@bristol.ac.uk)

Received 28 September 2005

Published 28 October 2005

Online at [stacks.iop.org/JPhysCM/17/S3551](http://stacks.iop.org/JPhysCM/17/S3551)

## Abstract

We study the formation and growth of equilibrium clusters in a suspension of weakly charged colloidal particles and small non-adsorbing polymers. The effective potential is characterized by a short-range attraction and a long-range repulsion. The size, shape and local structure of the clusters are studied using three-dimensional particle microscopy. We observe a rapid growth in the mean cluster size and the average number of nearest neighbours approaching the gel boundary.

(Some figures in this article are in colour only in the electronic version)

## 1. Introduction

The van der Waals theory is the foundation for our current understanding of fluid structure and phase equilibria [1]. It predicts, for an interaction potential consisting of a short-range repulsion and a long-range attraction, a first-order transition (below  $T_c$ ) between a dilute vapour and a dense fluid or liquid. Here we consider the unusual situation which pertains when the ranges of the repulsive and attractive forces are interchanged.

Experiments [2–6], theory [7–10] and simulation [11–13] suggest that a combination of a very short-ranged attraction and a much longer-range repulsion leads to a highly nontrivial phase behaviour. At low densities, there is compelling evidence for the existence of a fluid phase of finite-sized *equilibrium* aggregates or clusters [2–4]. The size and shape of these clusters are expected [12] to be very sensitive to the relative range of the attractive and repulsive components ( $V_R(r)$ ) of the total interparticle potential. Estimates of the ground state energies of clusters of different sizes suggest that the equilibrium shape changes from spherical to linear as the cluster diameter exceeds the decay length of  $V_R(r)$  [12, 13]. In addition, recent experiments [6] have revealed that, at high densities, the competition inherent in this system can also stabilize new particle architectures. Three-dimensional confocal microscopy in a system of weakly charged colloidal spheres shows, at high densities, the formation of a macroscopically percolating gel composed of linear aggregates of face-sharing tetrahedra of particles. The colloidal particles are arranged in the motif of a helical spiral in which each particle is connected

to six neighbours, analogous to the structure first proposed by Bernal in his classic study of hard-sphere glasses [14].

In this paper, we present an experimental study of a carefully characterized model system of colloidal spheres. The particles interact through an effective potential which consists of a short-range attraction, generated by the exclusion of a non-adsorbing polymer, and a long-range screened electrostatic repulsion. We focus on what happens to the size and shape of the self-assembled clusters as the gel boundary is approached.

## 2. Experimental details

We use a well studied model system: random-coil polystyrene (radius of gyration  $r_g = 92$  nm) mixed with PMMA spheres (diameter  $\sigma = 1840$  nm) dispersed in a near-density- and near-index-matched mixture of 78:22% by weight cycloheptyl bromide and *cis*-decalin. The PMMA spheres were labelled with the dye DiIC<sub>18</sub> to make them visible by fluorescence microscopy. Exclusion of the non-adsorbing polymer from a region between two neighbouring particles generates a short-range attraction, the range and strength of which is controlled by  $r_g$  and the free polymer concentration  $\phi_p^*$ . For the cases studied here the width of the attractive range is roughly  $0.1\sigma$ . Measurements of the particle electrophoretic mobility using phase analysis light scattering revealed that the PMMA particles develop a small positive charge,  $Q \approx +145e$ , in the density-matched solvent used in this study. The Debye screening length was estimated from measurements of the solvent conductivity ( $170 \pm 30$  pS cm<sup>-1</sup>) as of the order of  $\kappa\sigma \approx 0.5$ .

Mixtures with different colloid ( $\phi_c$ ) and polymer concentrations ( $\phi_p^*$ ) were prepared and homogenized by extensive tumbling. To minimize decomposition and to ensure reproducibility all samples, once prepared, were stored in light-tight containers at 4 °C, prior to measurement. The size and internal structure of clusters were studied using laser scanning confocal microscopy. The suspensions were sealed in a cylindrical cell of  $\sim 50$   $\mu$ l volume. Three-dimensional confocal microscopy was used to distinguish between a phase of isolated clusters and the formation of a macroscopic percolating network of particles. Our observations are summarized in figure 1. To follow the transition between isolated clusters and a gel phase in detail we focus here on the sample sequence A–G, figure 1, at  $\phi_p^* = 0.95$ . A stack of typically 345 images, spaced by 0.16  $\mu$ m vertically, was collected from a representative volume of 73  $\mu$ m  $\times$  73  $\mu$ m  $\times$  55  $\mu$ m within each suspension. Each stack contained, depending on  $\phi_c$ , the images of between 1500 and 45 000 spheres. The images were analysed quantitatively using algorithms similar to those described in [15] to extract the three-dimensional coordinates of each sphere. The position of each sphere was measured with a precision of approximately 70 nm.

## 3. Data analysis

The number, size and shape of the clusters were identified from the coordinate list. We define particles which are ‘bonded’ to each other by their separation  $r$ . If  $r \leq r_0$ , where the cut-off distance  $r_0$  was identified with the position of the first minimum in the pair distribution function  $g(r)$ , then the particles were considered neighbours. Standard algorithms were used to partition particles into clusters of size  $s$  and to evaluate the cluster size distribution  $n_s$ . The second moment of the cluster distribution  $\langle s_2 \rangle$  was used to characterize the average cluster size [16],

$$\langle s_2 \rangle = \frac{\sum_s s^2 n_s}{\sum_s s n_s}. \quad (1)$$

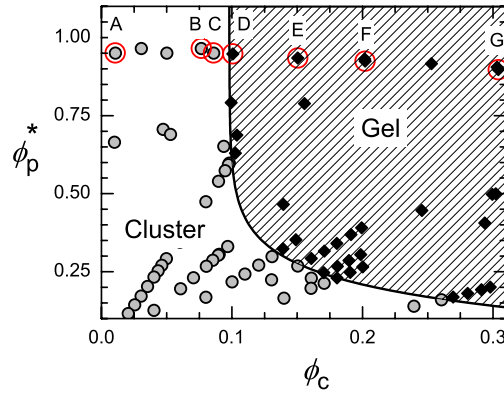


**Figure 1.** Behaviour of a charged colloid–polymer mixture. Circles represent samples that form isolated clusters. Diamonds depict macroscopic percolating gels. The solid line identifies the experimentally determined gel boundary  $\phi_g$ . Data from circled samples A–G are shown in figures 2–4.

The geometric properties of the clusters were evaluated from the eigenvalues  $\lambda_1 \leq \lambda_2 \leq \lambda_3$  of the radius of gyration tensor  $S$ , defined as

$$S_{\alpha\beta} = \frac{1}{2N^2} \sum_{i,j=1}^N [r_{i,\alpha} - r_{j,\alpha}][r_{i,\beta} - r_{j,\beta}] \quad (2)$$

with  $r_i$  the position of the  $i$ th sphere in the cluster of size  $N$  and  $(\alpha, \beta) = 1, 2, 3$  denoting the corresponding Cartesian components. We characterize the size and shape of the cluster in terms of the rotational invariants of the tensor  $S$ . The trace  $\sum_i \lambda_i$  gives the usual isotropic squared radius of gyration  $r_g^2$  while the anisotropy of the cluster is measured by the asphericity  $A_2$  [17],

$$A_2 = \frac{(\lambda_1 - \lambda_2)^2 + (\lambda_2 - \lambda_3)^2 + (\lambda_3 - \lambda_1)^2}{2(\lambda_1 + \lambda_2 + \lambda_3)^2}. \quad (3)$$

The asphericity is normalized so that  $A_2$  ranges from zero for a spherically symmetric cluster to one for a rod-like cluster.

#### 4. Results

The left panel of figure 2 shows the evolution in the proportion of *single* unbonded particles  $f$  as a function of  $\phi_c$ . The boundary between a non-percolating cluster phase and the percolating gel occurs at  $\phi_g \approx 0.1$ . The most striking feature is the abrupt change in the number of single particles approaching the gel boundary. At low colloid concentrations  $f$  is approximately constant at  $f \approx 0.22$ , independent of  $\phi_c$ —the remaining 78% of particles being incorporated into clusters. The proportion of single particles however drops rapidly in the gel phase, although it remains finite even for dense gels ( $f \approx 10^{-2}$  at  $\phi_c = 0.3$ , for instance). The coexistence evident in these samples between free and bonded particles highlights the dynamic nature of the assembly process. Direct visual observation showed a slow but continuous exchange of particles between clusters. Although the rates of exchange appeared to reduce with increasing number density, particles could still be seen joining and detaching from the chains of the gel phase. To provide further evidence that equilibrium had been reached we studied the time-dependence of  $f$ . We found no qualitative change in the period of a week, during which time particle sedimentation was negligible.

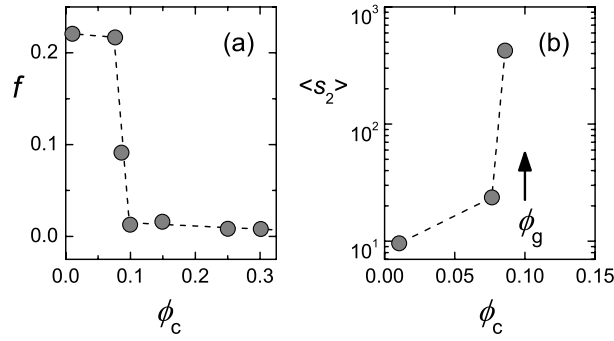


**Figure 2.** (a) The proportion of unbonded particles  $f$  and (b) the average cluster size  $\langle s_2 \rangle$ , as a function of colloid volume fraction  $\phi_c$ , for samples marked A–G in figure 1.

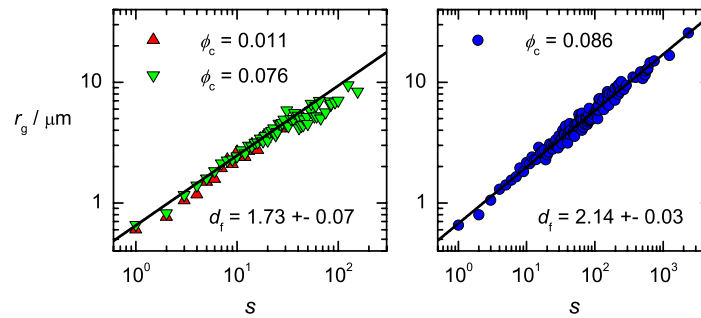


**Figure 3.** Size dependence of the cluster radius of gyration: sample A,  $\phi_c = 0.011$  (triangles), sample B,  $\phi_c = 0.076$  (inverted triangles), and sample C,  $\phi_c = 0.086$  (circles). The lines are power law fits to the data.

Figure 2(b) shows the growth in the average cluster size  $\langle s_2 \rangle$ , defined in equation (1), with increasing  $\phi_c$  for all non-percolating states. Clearly the average cluster size increases rapidly approaching the gel boundary. This rapid growth is mirrored in the number of particles  $s_{\text{max}}$  contained in the largest observed cluster, which increases from 37 ( $\phi_c = 0.011$ ) to 155 ( $\phi_c = 0.076$ ), to reach  $s_{\text{max}} = 2340$  at  $\phi_c = 0.086$ . To quantify these changes in greater detail we determined the size dependence of the ensemble-averaged radius of gyration  $\langle r_g \rangle$ . For fractal aggregates  $r_g$  displays a power law dependence on the number of particles  $s$ ,  $\langle r_g \rangle \sim s^{1/d_f}$ , where  $d_f$  is the fractal dimension. Figure 3 shows plots of  $r_g$  versus  $s$ , at three values of  $\phi_c$ . Interestingly, we find that at all densities the clusters show fractal scaling but that the fractal dimension  $d_f$  shows a marked dependence on  $\phi_c$ . At low  $\phi_c$ , the fractal dimension found of  $d_f = 1.73 \pm 0.07$  is consistent with the diffusion-limited cluster–cluster aggregation (DLCA) value in three dimensions ( $d_f = 1.78$  [18, 19]), while at high  $\phi_c$  the value of  $d_f = 2.14 \pm 0.03$  is consistent with the reaction-limited cluster–cluster aggregation (RLCA) value in three dimensions ( $d_f = 2.1$  [20]). This apparent crossover between DLCA and RLCA kinetics with  $\phi_c$  is unexpected. However, it is unclear if fractal models for non-equilibrium growth are applicable to the equilibrium case of assembly studied here for which, as we indicate below, the cluster shape is not truly self-similar.

A simple indicator of the anisotropy of the clusters is provided by the asphericity  $\langle A_2 \rangle$ , defined in (3). In contrast to the  $r_g$  data we find little  $\phi_c$  dependence of the average cluster asphericity, plotted in figure 4(a). Both low and high density samples show a similar monotonic

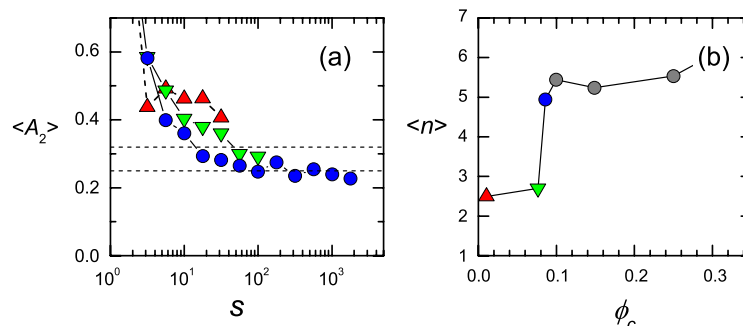


**Figure 4.** (a) Cluster asphericity as a function of cluster size. The dotted lines depict the asphericity expected for random percolation [21] and DLCA models [22]. (b) Average number of neighbours as a function of volume fraction  $\phi_c$ . Symbols have the same meaning as in figure 3.

decrease in  $\langle A_2 \rangle$  with  $s$ , consistent with a progressive change in shape with increasing cluster size. The clusters formed are therefore not self-similar. Clusters smaller than about 30–50 monomers show a definite tendency to be elongated in one dimension as evidenced by the increasing value of  $\langle A_2 \rangle$  found at small  $s$ . This preference for a linear or rod-like shape seems to be more pronounced the smaller the cluster. These observations are supported by images of individual clusters which reveal characteristic one-dimensional bundles of particles. By contrast, while large clusters remain anisotropic the levels of asymmetries are significantly lower and typical of clusters formed from either random percolation ( $\langle A_2 \rangle = 0.25$  [21]) or DLCA models ( $\langle A_2 \rangle = 0.32$  [22]). This crossover suggests that in large clusters the short one-dimensional bundles have branched many times, generating clusters with geometries controlled by random percolation.

The tendency seen for one-dimensional aggregation at short scales might indicate that the cluster is constructed locally from segments of Bernal spiral structures. To check for this possibility, we calculated the average number of nearest neighbours  $\langle n \rangle$ . As shown in figure 4(b),  $\langle n \rangle$  grows abruptly with increasing  $\phi_c$  approaching the gel boundary. Above  $\phi_g$ , the mean coordination number is insensitive to  $\phi_c$  and is approximately six, consistent with the characteristic sixfold coordination of a Bernal spiral. Moreover, figure 4 reveals that  $\langle n \rangle$  is less than six in the non-percolating cluster samples (A–C). This is particularly evident in sample B ( $\phi_c = 0.076$ ), which while it contains clusters of up to 100 monomers has a mean coordination number of only  $\langle n \rangle = 2.7$ . The lack of spiral ordering, shown by the low values of  $\langle n \rangle$ , is also supported by direct inspection which reveals little evidence for Bernal ordering in any of the non-percolating cluster samples.

## 5. Conclusions

In this work we have explored the change in the size and shape of the clusters formed in a colloidal system of short-range attractions and long-range repulsions, approaching the gelation transition. In contrast to a purely attractive system the clusters are equilibrium entities and their properties time independent. Our most noteworthy finding is that the average size ( $s_2$ ) of the cluster distribution, the proportion of unattached particles, and the mean coordination number all change abruptly as  $\phi \rightarrow \phi_g$ . Although we have studied only a limited number of concentrations (at one specific choice of potential parameters) these observations suggest that, for this system, gelation has many of the hallmarks of an *equilibrium* transition. Qualitatively,

our observations appear consistent with the suggestion by Groenewold and Kegel [7, 8] that under the right conditions a fluid of isolated clusters will undergo a spinodal decomposition, driven by counter-ion condensation, to form a macroscopic gel. This raises the enticing possibility of an ideal thermally reversible gel—one in which the gel-line might be approached infinitely closely and the dynamics of arrest studied precisely and reproducibly, free from the dynamical complications of purely attractive systems. Further experiments are planned to test these ideas.

### Acknowledgments

It is a pleasure to thank Drs A I Cambell, J S van Duijneveldt, M Faers and Adele Donovan for assistance. This work was supported financially by EPSRC and MCRTN-CT-2003-504712.

### References

- [1] Widom B 1967 *Science* **157** 375
- [2] Segre P N, Prasad V, Schofield A B and Weitz D A 2001 *Phys. Rev. Lett.* **86** 6042
- [3] Sedgwick H, Egelhaaf S and Poon W C K 2004 *J. Phys.: Condens. Matter* **16** S4913
- [4] Stradner A, Sedgwick H, Cardinaux F, Poon W C K, Egelhaaf S and Schurtenberger P 2004 *Nature* **432** 492
- [5] Bordi F, Cametti C, Diociaiuti M and Sennato S 2005 *Phys. Rev. E* **71** 050401(R)
- [6] Campbell A I, Anderson V J, van Duijneveldt J S and Bartlett P 2005 *Phys. Rev. Lett.* **94** 208301
- [7] Groenewold J and Kegel W K 2001 *J. Phys. Chem. B* **105** 11702
- [8] Groenewold J and Kegel W K 2004 *J. Phys.: Condens. Matter* **16** S4877
- [9] Wu J, Liu Y, Chen W-R, Cao J and Chen S-H 2004 *Phys. Rev. E* **70** 050401
- [10] Liu Y, Chen W-R and Chen S-H 2005 *J. Chem. Phys.* **122** 044507
- [11] Sciortino F, Mossa S, Zaccarelli E and Tartaglia P 2004 *Phys. Rev. Lett.* **93** 055701
- [12] Mossa S, Sciortino F, Tartaglia P and Zaccarelli E 2004 *Langmuir* **20** 10756
- [13] Sciortino F, Tartaglia P and Zaccarelli E 2005 *Preprint cond-mat/0505453*
- [14] Bernal J D 1964 *Proc. R. Soc. A* **280** 299
- [15] Crocker J C and Grier D G 1996 *J. Colloid Interface Sci.* **179** 298
- [16] Stauffer D 1985 *Introduction to Percolation Theory* (London: Taylor and Francis)
- [17] Rudnick J and Gaspari G 1986 *J. Phys. A: Math. Gen.* **19** L191
- [18] Weitz D A, Huang J S, Lin M Y and Sung J 1985 *Phys. Rev. Lett.* **54** 1416
- [19] Meakin P 1989 *J. Colloid Interface Sci.* **102** 491
- [20] Lin M Y, Lindsay H M, Weitz D A, Ball R C, Klein R and Meakin P 1990 *Phys. Rev. A* **41** 2005
- [21] Aronovitz J A and Stephens M J 1987 *J. Phys. A: Math. Gen.* **20** 2539
- [22] Fry D, Mohammad A, Chakrabarti A and Sorensen C M 2004 *Langmuir* **20** 7871